Online Appendices for:

Effects of climate change on an emperor penguin population: analysis of coupled demographic and climate models

Stéphanie Jenouvrier[1,2,4,5],
Marika Holland[3],
Julienne Strœve[4],
Christophe Barbraud[2],
Henri Weimerskirch[2],
Mark Serreze[4,5],
Hal Caswell[1,6]

May 1, 2012

1. Biology Dept., MS-34, Woods Hole Oceanographic Institution, Woods Hole, MA 02543, USA,

2. Centre d'Etudes Biologiques de Chizé, Centre National de la Recherche Scientifique, F-79360 Villiers en Bois, France,

3. Oceanography Section, National Center for Atmospheric Research, Boulder, 80305 CO, USA,

4. National Snow and Ice Data Center, Boulder, 80309 CO, USA

5. Cooperative Institute for Research in Environmental Science, University of Colorado Boulder, 80309-0449, USA

6. Max Planck Institute for Demographic Research, Rostock, Germany.

Contents

1 Appendix 1: Density dependence effects

A reviewer questioned the effect of density dependence on emperor penguin population in Terre Adélie. We have a priori reasons for expecting density effects to be small in this population.

The emperor penguin population in Terre Adélie decreased by 50% during the mid-70s, and remained stable since then (Barbraud & Weimerskirch 2001; Jenouvrier *et al.* 2005b). If this population were having a dramatic effect on its environment, then population decline should be followed by improved conditions. If these effects mattered, they should be apparent in per capita growth rates following a population reduction, and would be apparent after conditions returned to normal after 50% population decrease. This did not happen.

Moreover, as always, "density" dependence is shorthand for resource dependence. The emperor penguin interacts with a complex food web, over wide spatial scale, differentially among life cycle stages and seasons of the year. Breeding and non-breeding individuals occupy very different environments. The environment[s] fluctuate[s] dramatically over time. Unlike density, these fluctuations have readily detectable effects on population (e.g., sea ice shows a well-known periodicity around 3- 5 years, which corresponds to the periodicity of the emperor penguin population size, Jenouvrier *et al.* (2005b)).

Previous examinations of density dependence in this population (Barbraud & Weimerskirch 2001; Jenouvrier *et al.* 2005a) actually found a positive effect of population size on adult survival during the entire period of the study (ie. 1962- 2000). This positive relationship may result from penguin behavior: huddling together in groups for protection from the harsh Antarctic winter during the breeding season. However, even this relationship is unclear and may depend on sexes and sea ice conditions. Gimenez & Barbraud (2009), in a paper exploring a new methodology, found a non-linear effect of population size on adult survival, which interacted with sea ice conditions. However, because their paper was methodological, their analysis did not included any model selection.

In Supplementary Appendix 3, we have re-analysed the effect of population size on adult

survival during the time period of the present study (i.e from 1979 to 2000). The model is not supported by our model selection (deltaAIC=12.80 for a covariate based on the number of breeding pairs and deltAIC=13.82 for a covariate based on the population growth, both AIC weights are null).

2 Appendix 2: Principal component analysis of sea ice variables

We first explore thoroughly different potential environmental covariates affecting the emperor life cycle (Ainley *et al.* 2010) including sea ice concentration (SIC) and extent (SIE), indices of fast ice area and polynya size. We do not include sea ice thickness because satellite data time series are very short. Our selected environmental variables are highly correlated at our large spatial scale. Thus, we use a set of principal component analysis to obtain a reduced and uncorrelated set of environmental variables for several seasons of the emperor life cycle.

The first principal component of all the analysis accounts for most of the variability in the data ($> 60\%$, Table 1) and is strongly related to SIC. Therefore we restrict our study to SIC, which is a well known and studied environmental variable.

Table 1 shows the strong correlations between our preliminary selected variables and SIC. As SIC increases, SIE and the area of fast ice increase during the various seasons. As SIC increases, the polynya size increases during summer (non- breeding and creche seasons) while it decreases during winter. During summer, the area covered by sea ice is limited and the maximum sea ice extent is likely within the spatial sector considered. Thus when the sea ice forms and the area covered by sea ice (i.e. SIC) increases, the area of open water within sea ice (i.e. polynya) increases. During winter, most of the area around the penguin colony is covered by sea ice and the limit with the open ocean is likely outside the spatial sector considered. Thus when the area covered by sea ice decreases, the area of open water within sea ice increases.

In this preliminary analysis we explored six seasons of the penguin life cycle but restricted further our analysis to four seasons for again limiting correlations between covariates.

Table 1: Preliminary analysis to select environmental covariates. The first column represents the season of the emperor penguin life cycle for which the environmental analysis is conducted. The second column shows the percent of variance in all the covariates accounted by the first principal component. The following columns represent the Pearson correlation coefficients among the environmental covariates (sea ice extent (SIE), indices of fast ice area and polynya size) and sea ice concentration (SIC). The p-values of all relationships are < 0.05 except the one in italic.

Season	% variance	SIE	Fast	Polynya
Non- breeding	85	0.98	0.87	0.66
Laying	70	*0.35*	0.58	-0.72
Incubating	69	0.58	0.89	-0.96
Brooding	61	0.42	0.89	-0.90
Creche	60	0.55	0.60	-0.94
Departure	79	0.75	NaN	0.71

We calculated sea ice concentration (SIC) anomalies, relative to 1979–2007 (SIC_a) as:

$$x_t = \frac{z_t - \overline{z}}{\overline{z}} \tag{1}$$

where z_t is SIC in year t and $\overline{z}$ the mean of SIC from 1979 to 2007. We consider four seasons of the emperor life cycle, and define the vector $\mathbf{x}_t$ whose elements are the values of SIC_a during the non-breeding, laying, incubating and rearing.

Figure 1 shows the observed SIC_a values during each season; the values are extremely variable, especially during the nonbreeding season.

Values of SIC_a during different seasons are still correlated (Table 2). We use principal component analysis to obtain a reduced and uncorrelated set of sea ice variables. We analyze standardized SIC_a (i.e x_t/σ_x with σ_x the standard deviation of SIC_a) because SIC_a is much more variable during the non-breeding season than SIC_a during the breeding season (Fig. 1). The first two principal components explain 78% of the variance (respectively 56% and 26%).

Table 3 contains the coefficients of the first two principal components. The coefficients of the first principal component (PC1) have the same sign, making it a weighted average of all the original variables, with most of the emphasis on the breeding season. We call PC1 the annual SIC_a. The second principal component (PC2) contrasts the non-breeding season and the breeding season (positive versus negatives coefficients respectively). We call PC2 the seasonal difference in SIC_a.

Figure 2 show SIC_a during the various seasons as function of PC1 and PC2, with PC3 and PC4 set equal to zero. They are calculated as $\mathbf{x} = \text{diag}\,(\boldsymbol{\sigma})\mathbf{C}\mathbf{p}$, where $\boldsymbol{\sigma}$ is a vector containing the standard deviations of SIC_a in each season, $\mathbf{C}$ is a matrix containing the principal component coefficients as rows, and $\mathbf{p}$ is a vector containing the values of $PC1, \ldots, PC4$.

From Figure 2a, when annual SIC_a increases, SIC_a during the various seasons increase with similar rates during the breeding season and a higher rate during the non-breeding season. When the seasonal difference in SIC_a increases, SIC_a during the non-breeding

season decrease, while SIC_a during incubation and rearing slightly increase (Fig. 2b).

Table 2: Pearson correlation coefficients among SIC_a values for the four seasons of the penguin life cycle. Star indicates that $P < 0.05$.

SIC_a	laying	incubating	rearing
nonbreeding	0.4747*	0.1441	0.2611
laying		0.6159*	0.4405*
incubating			0.4807*

Table 3: Coefficients of the principal component analysis. They represent the linear combinations of the SIC_a that generate the two first principal components.

SIC_a	PC 1	PC 2
non breeding	0.386	0.8358
laying	0.581	0.09
incubating	0.5229	-0.4775
rearing	0.4899	-0.2556

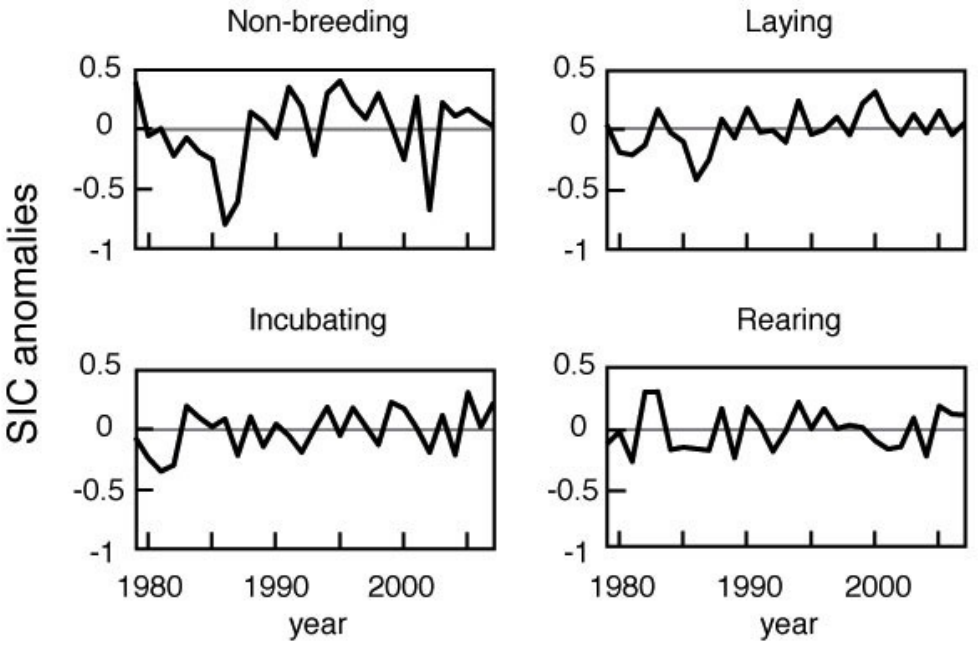

Figure 1: Observed proportional anomalies in sea ice concentration (SIC) relative to the mean from 1979 to 2007, for each of four seasons of the penguin life cycle. The grey line shows $SIC_a = 0$ and represents the mean SIC from 1979 to 2007.

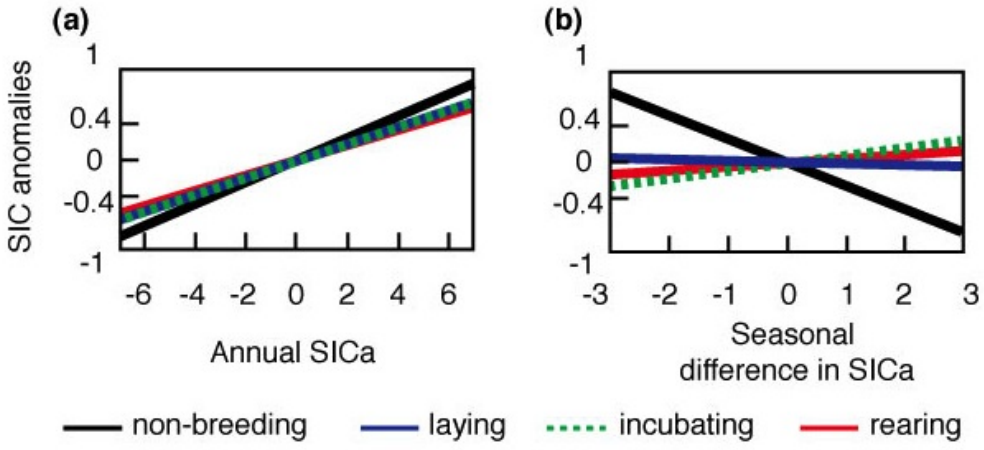

Figure 2: (a) Seasonal SIC anomalies as a function of the annual SIC_a, with the seasonal differences in SIC_a set to zero. (b) Seasonal SIC anomalies as a function of the seasonal differences in SIC_a, with the annual SIC_a set to zero.

3 Appendix 3: Vital rates

3.1 Breeding success

To study the effect of seasonal sea ice anomalies during the four seasons on breeding success, we apply a General Linear Mixed Model with a logistic link function and random year effects. Table 4 shows that the best model supported by the data is a negative effect of SIC_a during the rearing season.

Table 4: Results of the General Linear Mixed Model analysis for the breeding success. The first column shows the various seasons of the emperor penguin life cycle. The second column describes the type of relationship on the logit scale and the third column is the Bayesian information criterion for the fitted model. The model selected shows the lowest BIC. The following columns represent the estimates with their standard error (β_0 is the intercept and β_1 and β_2 are the slopes).

seasons	relationship	BIC	β_0	β_1	β_2
laying	linear	8.61	0.06 ± 0.17	-0.86 ± 1.07	
	quadratic	11.23	-0.04 ± 0.20	-0.72 ± 1.11	4.29 ± 5.03
incubating	linear	9.18	0.06 ± 0.17	0.27 ± 0.97	
	quadratic	11.27	-0.12 ± 0.23	0.49 ± 0.99	6.14 ± 5.63
SIC rearing	linear	7.65	0.07 ± 0.16	-1.25 ± 0.99	
	quadratic	10.24	0.22 ± 0.24	-1.05 ± 1.01	-5.66 ± 6.44

3.2 Adult survival

Table 5 and 6 detail the result of model selection. Our analysis includes freely time variations models, time-invariant models and covariates models. Among covariates we tested effect of sea ice concentration anomalies (SIC_a) over the four seasons of the emperor penguin life cycle, and the effect of population size and growth to study the effect of density dependence.

Previous studies using a rigorous model selection have shown a positive effect of population size on adult survival (Barbraud & Weimerskirch 2001; Jenouvrier *et al.* 2005a). Indeed, on the breeding grounds, the effect of density may be positive because the breeding population relies on group defense (form huddle against the coldest environment on earth).

Previous studies have also shown that models with environmental variables were more supported than a model with population size. Likewise, we show here that population size or growth models are not supported (null AIC weights, Table 6). Therefore, we do not include density dependence in our population model.

Adult survival probabilities are strongly affected by seasonal SIC_a for both sexes, and models with SIC_a during the breeding seasons appear in the top models. Figure 3 shows adult survival as function of annual sea ice and seasonal differences in sea ice, which account for most of the varialibility in SIC_a during the four seasons (Appendix 1). It details the uncertainties around adult survival estimates resulting from model selection and estimation error. Table 7 describes parameter estimates and their associated error.

3.3 Probabilities of return to the colony

It would be reasonable to expect an indirect effect of SIC_a on the probability that a breeder will return to breed the following year, because the cost of reproduction might be higher (due to longer foraging trips) in a year with high SIC_a. However, the CMR model analysis does not support any effect of SIC_a on the probability of return to the colony for breeders (Table 9). Models with freely time-varying return probabilities are highly supported, for both breeders and nonbreeders (Table 8, 9, Fig 4).

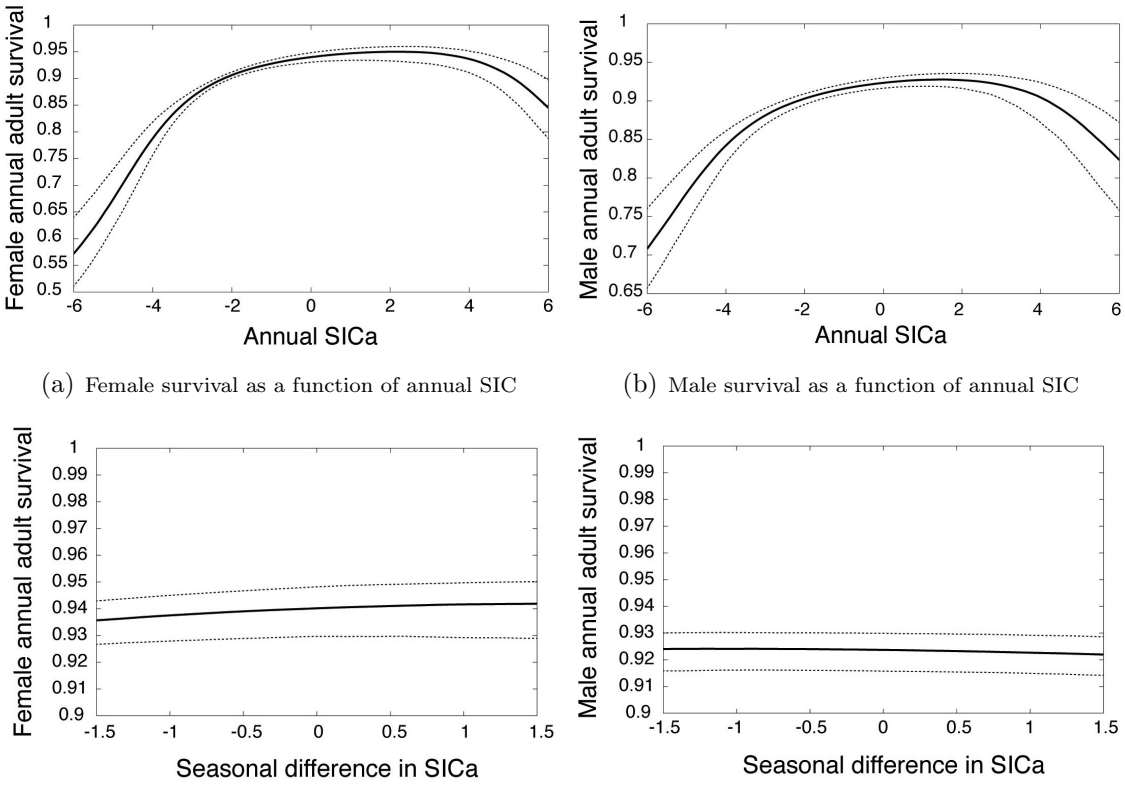

(a) Female survival as a function of annual SIC

(b) Male survival as a function of annual SIC

(c) Female survival as a function of seasonal SIC

(d) Male survival as a function of seasonal SIC

Figure 3: Annual adult survival as a function of annual SIC_a and seasonal differences in SIC_a. Right and left panels show the survival of females and males respectively. Upper panels show survival as a function of annual SIC_a for null values of seasonal differences in SIC_a. Lower panels show survival as a function of seasonal differences in SIC_a for null values of annual SIC_a. Dotted lines are the 95% confidence intervals.

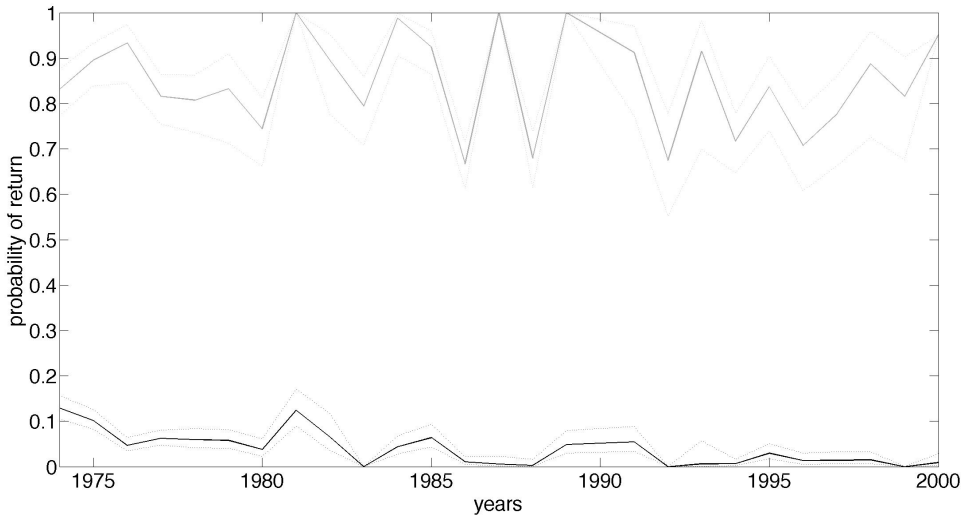

Figure 4: Probabilities of returning to the colony to breed. The black line refers to the return probability of non-breeders and the grey line to the return probability of breeders. Dotted lines show the 95% confidence intervals.

Table 5: Results of model selection for annual adult survival, including linear or quadratic effects of SIC_a at each of four seasons: non-breeding, laying, incubating and rearing. The first and second columns give the effects included in the model for females and males respectively. The number of parameters in the model is K, DEV is the deviance, AIC is the Akaikes information criterion, ΔAIC is the difference in Akaikes information criterion (AIC) between each model and the model with the smallest AIC (i.e. best supported by the data). AIC weights (AIC_w) represent the relative likelihood of a model and are used to create the averaged model. Only models for which the cumulative sum of AIC weights ($\sum AIC_w$) is 0.98 are included in model averaging.

Female	*Male*	K	DEV	AIC	ΔAIC	AIC_w	$\sum AIC_w$
incubating	*incubating*	135	39275.22	39545.22	0.00	0.14	0.136
$rearing^2$	$rearing^2$	137	39272.01	39546.01	0.78	0.09	0.227
$rearing^2$	*incubating*	136	39274.39	39546.39	1.17	0.08	0.303
incubating	$incubating^2$	136	39274.47	39546.47	1.25	0.07	0.376
$rearing^2$	*time -invariant*	135	39276.82	39546.82	1.59	0.06	0.437
$rearing^2$	$incubating^2$	137	39273.34	39547.34	2.11	0.05	0.484
rearing	*time-invariant*	134	39279.45	39547.45	2.22	0.04	0.529
rearing	*incubating*	135	39277.68	39547.68	2.46	0.04	0.568
$rearing^2$	*nonbreeding*	136	39277.52	39548.19	2.97	0.03	0.599
rearing	*laying*	135	39278.15	39548.33	3.10	0.03	0.628
incubating	*laying*	135	39280.03	39548.65	3.42	0.02	0.652
$rearing^2$	*rearing*	136	39276.76	39548.76	3.53	0.02	0.675
rearing	*nonbreeding*	135	39279.16	39548.83	3.60	0.02	0.698
time-invariant	*time-invariant*	133	39282.85	39548.85	3.63	0.02	0.720
rearing	$rearing^2$	136	39276.94	39548.94	3.71	0.02	0.741
incubating	*time-invariant*	134	39280.96	39548.96	3.73	0.02	0.762
$rearing^2$	*laying*	136	39277.22	39549.22	4.00	0.02	0.781
rearing	*rearing*	135	39279.34	39549.34	4.12	0.02	0.798
incubating	$rearing^2$	136	39277.35	39549.35	4.13	0.02	0.815
incubating	*rearing*	135	39279.36	39549.36	4.14	0.02	0.832
rearing	$incubating^2$	136	39277.37	39549.37	4.15	0.02	0.849
laying	*time-invariant*	134	39281.47	39549.47	4.25	0.02	0.865
time-invariant	*incubating*	134	39281.68	39549.68	4.46	0.01	0.880
laying	*incubating*	135	39279.74	39549.74	4.52	0.01	0.894
nonbreeding	*time-invariant*	134	39281.93	39549.93	4.70	0.01	0.907
time-invariant	*nonbreeding*	134	39282.21	39550.21	4.99	0.01	0.918
incubating	*nonbreeding*	135	39280.71	39550.71	5.49	0.01	0.927
incubating	$rearing^2$	136	39278.72	39550.72	5.50	0.01	0.936
rearing	$incubating^2$	136	39278.85	39550.85	5.63	0.01	0.944
time-invariant	$incubating^2$	135	39280.96	39550.96	5.74	0.01	0.952
laying	$incubating^2$	136	39278.97	39550.97	5.75	0.01	0.959
$incubating^2$	$rearing^2$	137	39277.32	39551.32	6.10	0.01	0.966
time-invariant	*laying*	134	39283.53	39551.53	6.31	0.01	0.971
laying	$rearing^2$	136	39279.56	39551.56	6.34	0.01	0.977

Table 6: Models for which the cumulative sum of AIC weights ($\sum AIC_w$) is > 0.98. Same legends as Table 5.

Female	*Male*	K	DEV	AIC	ΔAIC	AIC_w	$\sum AIC_w$
incubating^2	*incubating*^{2}	137	39277.68	39551.68	6.46	0.01	0.983
time-invariant	*rearing*	134	39283.70	39551.70	6.48	0.01	0.988
time-invariant	*rearing*^{2}	135	39282.41	39552.41	7.19	0.00	0.992
nonbreeding	*incubating*	135	39282.47	39552.47	7.25	0.00	1.00
nonbreeding	*rearing*^{2}	136	39281.42	39553.42	8.20	0.00	1.00
nonbreeding	*incubating*^{2}	136	39281.48	39553.48	8.26	0.00	1.00
Population size	*Population size*	135	39288.02	39558.02	12.80	0.00	1.00
Population growth	*Population growth*	135	39289.04	39559.04	13.82	0.00	1.00
freely time varying	*time-invariant*	153	39266.75	39570.57	25.35	0.00	1.00
time -invariant	*freely time varying*	153	39276.50	39578.07	32.84	0.00	1.00

Table 7: Parameters estimates of top models for annual adult survival, including linear or quadratic effects of SIC_a at each of four seasons: non-breeding, laying, incubating and rearing. The first column gives the effects included in the model for females and males respectively. The model order is the same than in main Table 1 and Appendix 2 Table 5. The following columns show estimates and standard error of the: intercept (β_0) and slopes of the relationships with sea ice (β_2 is the quadratic term).

covariate	$\beta_0 \pm se\beta_0$	$\beta_1 \pm se\beta_1$	$\beta_2 \pm se\beta_2$
Female			
incubating	2.70 ± 0.27	2.96 ± 1.25	
$rearing^2$	3.45 ± 0.30	2.28 ± 0.96	-17.99 ± 3.94
$rearing^2$	3.21 ± 0.51	2.48 ± 1.17	-13.32 ± 7.43
incubating	2.67 ± 0.27	2.93 ± 1.23	
$rearing^2$	3.01 ± 0.42	2.09 ± 1.10	-10.41 ± 6.33
$rearing^2$	3.23 ± 0.49	2.25 ± 1.05	-15.21 ± 7.19
rearing	2.69 ± 0.45	2.82 ± 2.59	
rearing	2.97 ± 0.89	4.41 ± 4.74	
$rearing^2$	3.00 ± 0.40	2.08 ± 1.08	-10.35 ± 6.18
rearing	2.81 ± 0.55	3.54 ± 3.06	
incubating	2.54 ± 0.21	1.88 ± 1.03	
$rearing^2$	3.01 ± 0.41	2.07 ± 1.15	-10.71 ± 6.26
rearing	2.69 ± 0.46	2.92 ± 2.65	
time-invariant	2.36 ± 0.15		
rearing	3.57 ± 1.02	7.32 ± 4.81	
incubating	2.53 ± 0.21	1.72 ± 1.03	
Male			
incubating	2.56 ± 0.28	2.73 ± 1.38	
$rearing^2$	3.10 ± 0.28	0.98 ± 0.94	-15.00 ± 3.96
incubating	2.55 ± 0.28	2.05 ± 1.41	
$incubating^2$	2.60 ± 0.25	1.26 ± 1.72	-5.69 ± 5.87
time-invariant	2.33 ± 0.16		
$incubating^2$	2.67 ± 0.27	0.17 ± 1.47	-8.56 ± 5.91
time-invariant	2.34 ± 0.18	$\pm$	
incubating	2.55 ± 0.32	1.72 ± 1.45	
nonbreeding	2.35 ± 0.17	0.42 ± 0.50	
laying	2.47 ± 0.24	1.49 ± 1.25	
laying	2.35 ± 0.19	1.17 ± 1.16	
rearing	2.31 ± 0.17	-0.18 ± 1.18	
nonbreeding	2.37 ± 0.19	0.43 ± 0.53	
time-invariant	2.25 ± 0.15		
$rearing^2$	3.12 ± 0.62	1.59 ± 1.28	-12.47 ± 9.04
time-invariant	2.26 ± 0.15		

Table 8: Selection of the capture-recapture models for the probability to return to the colony for non-breeders. Here, K is the number of parameters of the model, ΔAIC is the difference in Akaikes information criterion (AIC) between each model and the model with the smallest AIC (i.e. best supported by the data). AIC weights represent the relative likelihood of a model and are used to create the averaged model.

Model	K	ΔAIC	AIC weight
time-invariant	75	331.37	0
freely time varying	104	0	1

Table 9: Selection of the capture- recapture models including seasonal sea ice effects on the return probability of breeders. Legend as in Table 1.

Model	K	ΔAIC	AIC weight
time-invariant	105	293.77	0,00
freely time-varying	131	0	1.00
laying	106	291.13	0.00
incubating	106	280.87	0.00
rearing	106	268.34	0.00

4 Appendix 4: Effect of sea ice variability on demography

Here, we detail the effect of variability of annual SIC_a on the demography of emperor penguin, to understand its effect on the stochastic population growth rate. We show that variance of annual SIC_a reduces the deterministic population growth rate when mean annual SIC_a is in a medium range, but increases it for extreme positive or negative values of mean annual SIC_a. For this discussion, we denote mean annual SIC_a by μ.

Figures 5, 6, and 7 show the distributions of annual SIC_a, breeding success, and male and female adult survival for females and males, along with the resulting distribution of the deterministic growth rate λ. This deterministic rate can be thought of as approximating the growth of the population between time t and $t+1$, although this is not always true (see below).

Figure 5 shows the case when $\mu = 0$. As variance in annual SIC_a increases, the distribution of breeding success becomes more even, and the distribution of adult survival becomes skewed toward lower values. The result is a shift in the distribution of λ to lower values, associated with the reduced $\log \lambda_s$ seen in Figure 5 of the paper.

Figures 6 and 7 show comparable results when μ is very positive ($\mu = 5$) or very negative ($\mu = -5$); in these case variance in annual SIC_a increases $\log \lambda_s$ (Figure 5 of the paper).

When $\mu = 5$, increasing variance increases the probability of higher breeding success and adult survival, thus increasing λ. When $\mu = -5$, higher variance increases the probability of higher adult survival and reduces the survival differences between females and males, thus increasing λ.

It is important to note that the reasoning from the effects of variance on the distribution of λ to its effects on $\log \lambda_s$ is only crudely approximate. The stochastic growth rate cannot be inferred from the eigenvalues of the matrices appearing in the stochastic model. Indeed, it is possible for the stochastic growth rate to be positive even though all those eigenvalues

are less than 1, and vice-versa (Caswell (2001), Example 14.1).

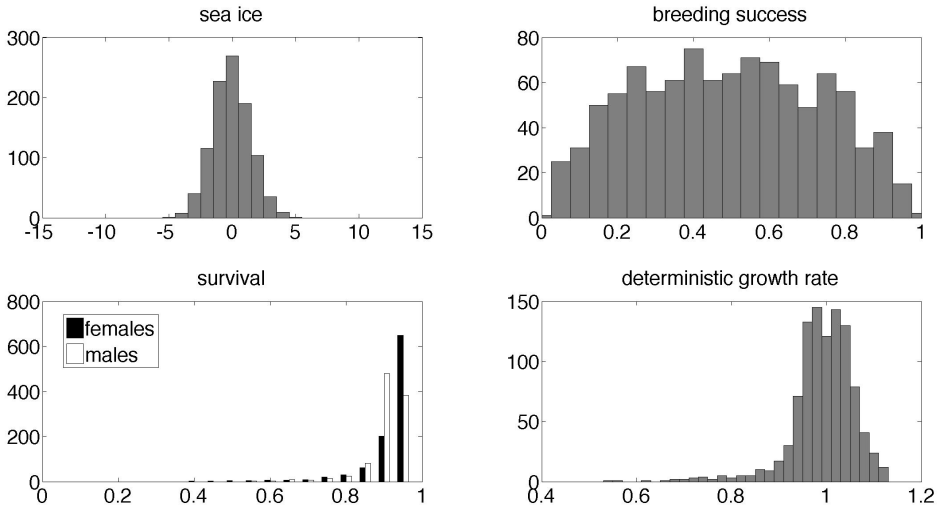

(a) $\mu = 0$ and $\sigma^2 = \sigma_o^2$

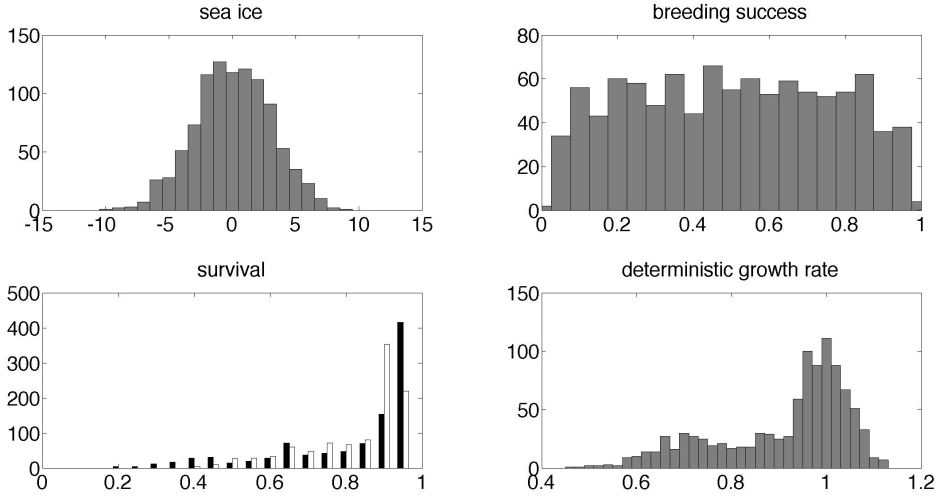

(b) $\mu = 0$ and $\sigma^2 = 2\sigma_o^2$

Figure 5: Effects of increased variance in annual SIC_a on the distributions of sea ice, adult survival, breeding success, and one-step deterministic population growth rates. The mean annual SIC_a is $\mu = 0$. In (a), the variance in annual SIC_a is equal to its observed value ($\sigma^2 = \sigma_o^2$). In (b), $\sigma^2 = 2\sigma_o^2$.

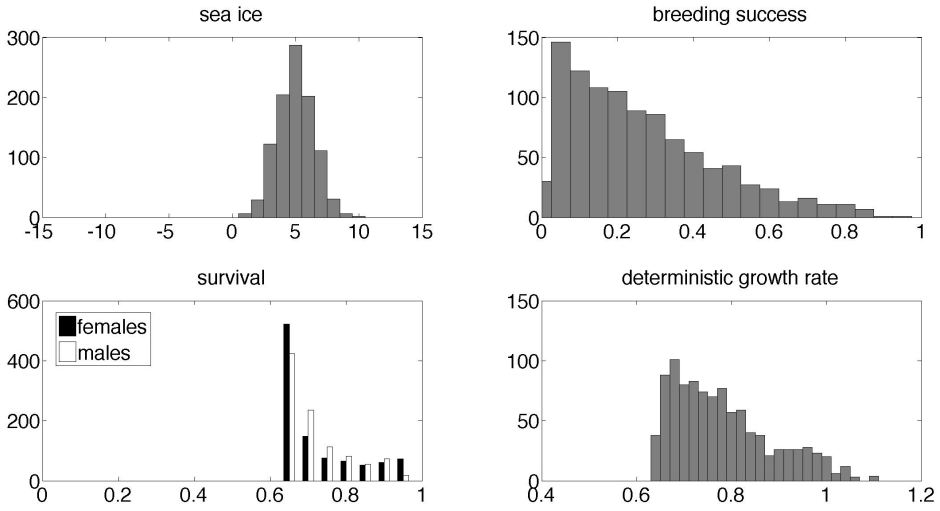

(a) $\mu = 5$ and $\sigma^2 = \sigma_o^2$

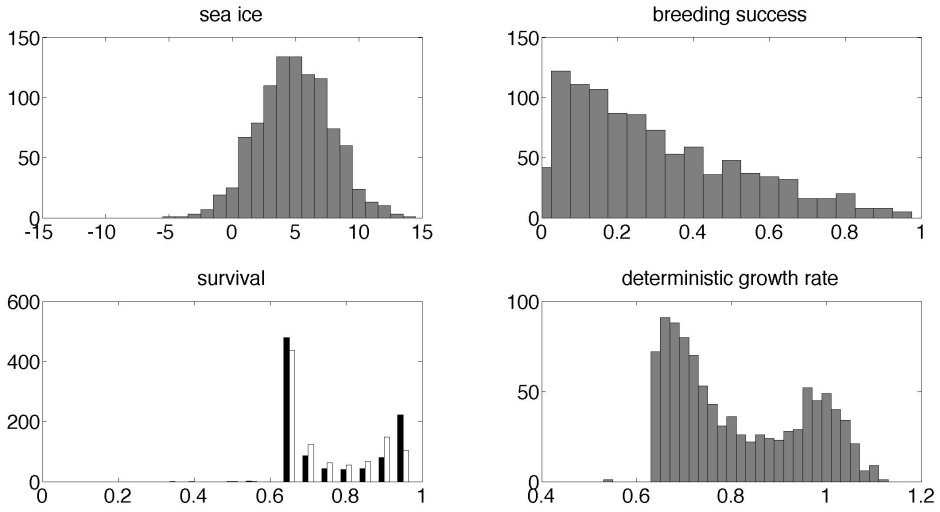

(b) $\mu = 5$ and $\sigma^2 = 2\sigma_o^2$

Figure 6: Effects of increased variance in annual SIC_a on the distributions of sea ice, adult survival, breeding success, and one-step deterministic population growth rates. The mean annual SIC_a is $\mu = 5$. In (a), the variance in annual SIC_a is equal to its observed value ($\sigma^2 = \sigma_o^2$). In (b), $\sigma^2 = 2\sigma_o^2$.

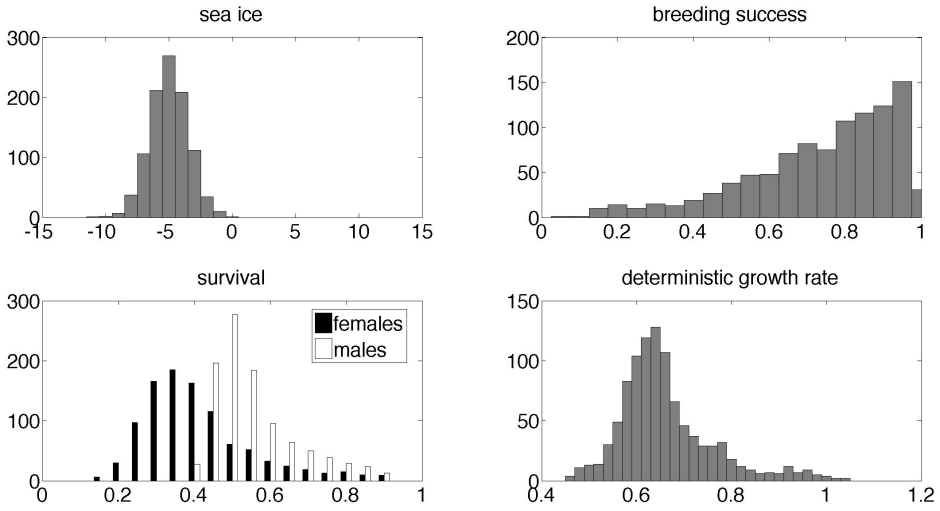

(a) $\mu = -5$ and $\sigma^2 = \sigma_o^2$

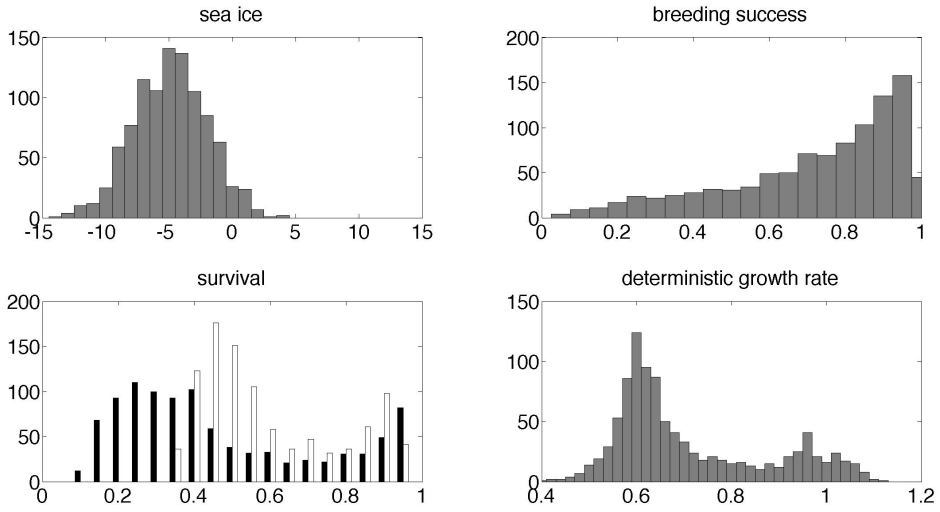

(b) $\mu = -5$ and $\sigma^2 = 2\sigma_o^2$

Figure 7: Effects of increased variance in annual SIC_a on the distributions of sea ice, adult survival, breeding success, and one-step deterministic population growth rates. The mean annual SIC_a is $\mu = -5$. In (a), the variance in annual SIC_a is equal to its observed value ($\sigma^2 = \sigma_o^2$). In (b), $\sigma^2 = 2\sigma_o^2$.

5 Appendix 5: Sea ice projected by climate models

5.1 Sea ice forecasts and climate model selection

Sea ice concentrations (SIC) are obtained from 20 General Circulation Models (GCMs) available as part as the WCRP CMIP3 multi-model dataset (http://esg.llnl.gov/portal) from the Program for Climate Model Diagnosis and Intercomparison (PCMDI) and the WCRP's Working Group on Coupled Modelling (WGCM). We calculate the SIC proportional anomalies relative to 1979- 2007 (SIC_a), in our region centered on Dumont D'Urville (DDU: 66°40 S 140°01 E) in Terre Adélie, using equation (1) of Appendix 1.

Figures 8, 9, 10, and 11 show the SIC_a forecasts from 1900 to 2100 obtained from these 20 GCMs, for the four seasons of the emperor penguin life cycle, as well as the SIC_a observed from 1979 to 2007. We eliminated the model giss-model-er because its spatial resolution is too coarse, and model iap-fgoals1-0-g because it produces nearly perpetual ice cover out to almost 40°S (Ainley et al. 2010, Ecological archives), resulting in a poor agreement between their SIC_a projections and observations.

To select from the remaining models a set for which the statistical properties of the SIC_a output agree well with the ones of observations from 1979 to 2007, we compared the median and standard deviation of the SIC_a distributions. First, we compare the medians, selecting model m if

$$Q_1 \leqslant \overline{\mathbf{x}_m} \leqslant Q_3 \tag{2}$$

where $\overline{\mathbf{x}_m}$ is the median of the SIC_a output of model m and Q_1 and Q_3 are the first and third quartile of the distribution of observations. Then we compare the standard deviation of SIC_a, selecting model m if

$$0.5 * \sigma_{\mathbf{x}_o} \leqslant \sigma_{\mathbf{x}_m} \leqslant 1.5 * \sigma_{\mathbf{x}_o} \tag{3}$$

where $\sigma_{\mathbf{x}_m}$ and $\sigma_{\mathbf{x}_o}$ are the standard deviation of SIC_a from climate model m and from

observations respectively. Our final ensemble of models are those that pass both tests during all four seasons.

These criteria tend to choose models with small root mean square error (RMSE) between observations and predictions, where

$$RMSE_m = \sqrt{\sum_y (x_{my} - x_{oy})^2 / n} \tag{4}$$

where x is the SIC_a during the various seasons, y the year and n the number of years. A RMSE of zero, means that the IPCC forecast projects SIC_a observations with perfect accuracy. Table 10 shows the results. The selected set of models are among those with the lowest RMSE, supporting our choice of criteria. The model ncar-ccsm3-0 also has a low RMSE; it passed all our criteria except during the incubating season, during which its variability was too low (see Fig. 10).

5.2 Stochastic sea ice forecasts

As described in the text, we generated stochastic forecasts of SIC_a, from the smoothed mean and covariances of the four-dimensional SIC_a values. Figure 12 illustrates the smoothed mean of SIC_a using different smoother parameters, and the resulting SIC_a forecasts. As the smoothing parameter h increases, fluctuations in the means and variances are reduced and the resulting stochastic forecasts are blurry. We choose $h = 2$, which introduce stochasticity in climate forecasts but retains the pattern of the original trajectory of GCMs forecast reasonably well (Fig. 12).

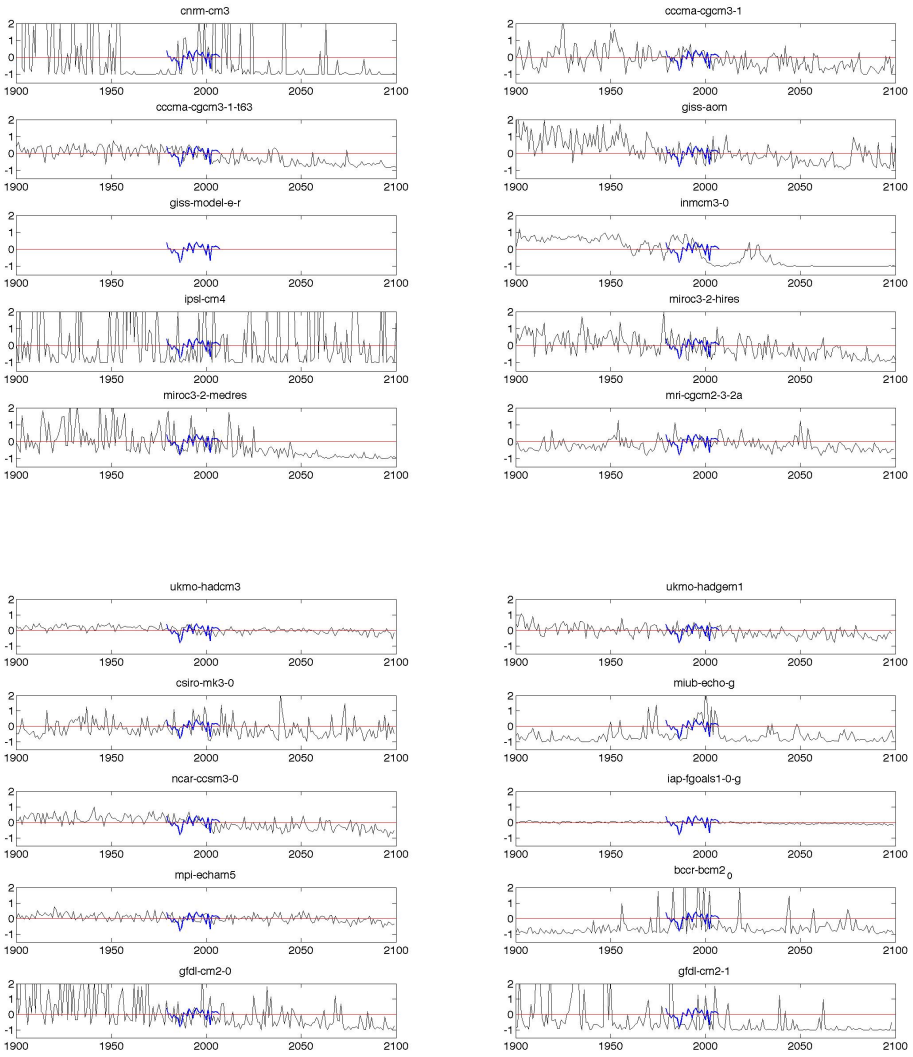

Figure 8: Forecasts of sea ice concentrations proportional anomalies relative to 1979- 2007 (SIC_a) from 1900 to 2100 from 20 GCMs (black line) and SIC_a observed from 1979 to 2007 with satellite (blue line) during the non-breeding season of emperor penguins. The red line refers to $SIC_a = 0$, i.e SIC equal to the present average.

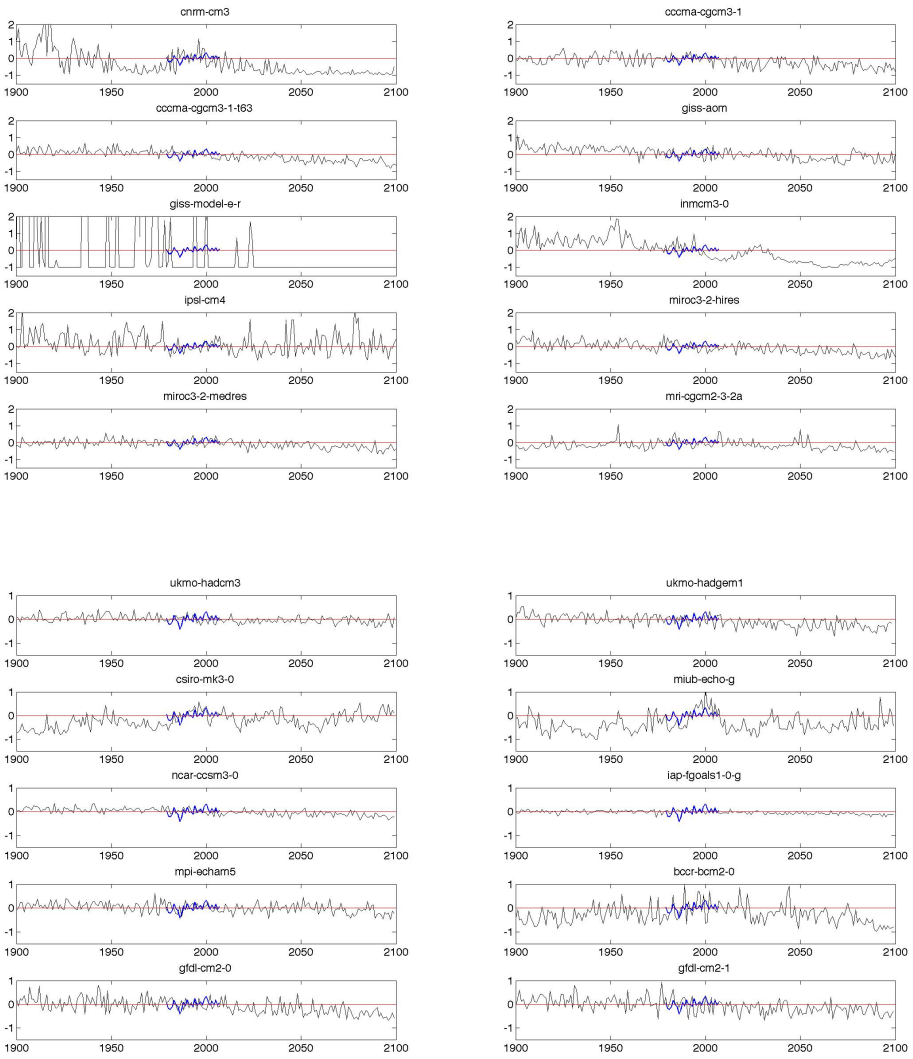

Figure 9: SIC_a forecasts from 1900 to 2100 for the 20 GCMs (black line) and SIC_a observed from 1979 to 2007 with satellite (blue line) during the laying season of emperor penguins.

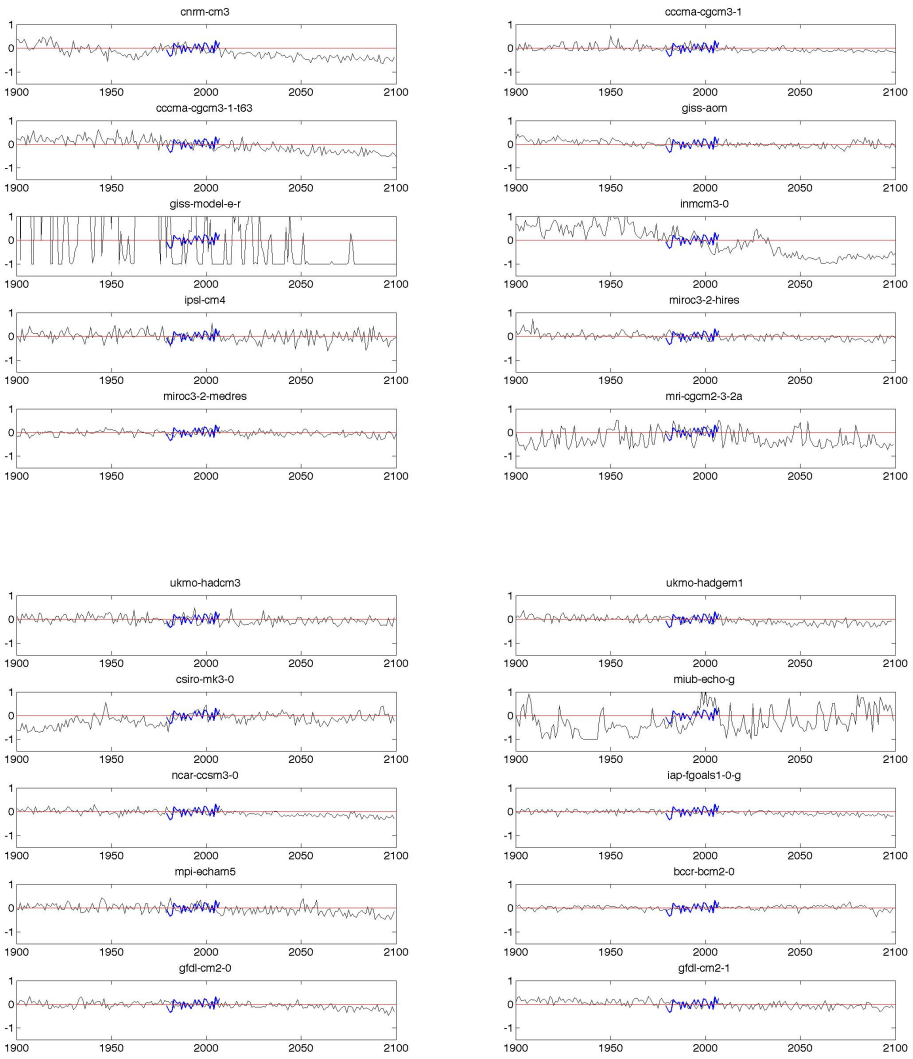

Figure 10: SIC_a forecasts from 1900 to 2100 for the 20 GCMs (black line) and SIC_a observed from 1979 to 2007 with satellite (blue line) during the incubating season of emperor penguins.

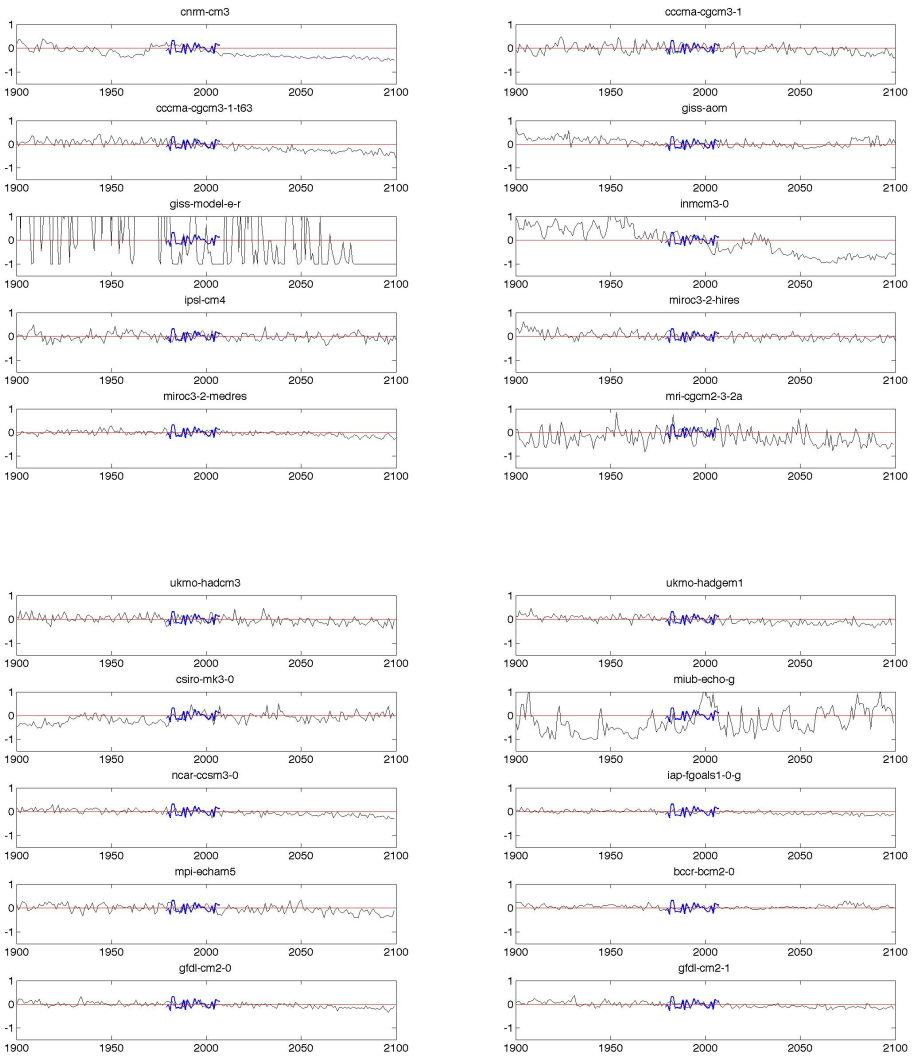

Figure 11: SIC_a forecasts from 1900 to 2100 for the 20 GCMs (black line) and SIC_a observed from 1979 to 2007 with satellite (blue line) during the rearing season of emperor penguins.

Table 10: The root mean square error (RMSE) measures the difference between SIC_a projected by a GCMs and SIC_a estimated from satellite observations. RMSE are calculated for each GCM and each season of the emperor penguin life cycle. MEAN refers to the averaged RMSE across the four seasons for each GCM. The GCMs selected in our analysis are highlighted in bold.

model	nonbreeding	laying	incubating	rearing	MEAN
ukmo-hadcm3	0.37	0.21	0.25	0.23	0.26
ncar-ccsm3-0	0.48	0.19	0.19	0.20	0.26
mpi-echam5	0.40	0.23	0.28	0.23	0.29
ukmo-hadgem1	0.48	0.25	0.23	0.21	0.29
cccma-cgcm3-1	0.50	0.23	0.23	0.22	0.29
cccma-cgcm3-1-t63	0.50	0.28	0.25	0.21	0.31
giss-aom	0.56	0.33	0.22	0.21	0.33
miroc3-2-medres	0.69	0.25	0.21	0.17	0.33
csiro-mk3-0	0.63	0.26	0.22	0.23	0.33
gfdl-cm2-0	0.75	0.27	0.23	0.20	0.36
mri-cgcm2-3-2a	0.52	0.31	0.32	0.34	0.37
miroc3-2-hires	0.71	0.34	0.25	0.21	0.38
inmcm3-0	0.78	0.44	0.36	0.32	0.47
bccr-bcm2-0	1.24	0.45	0.17	0.16	0.51
miub-echo-g	0.84	0.41	0.51	0.59	0.58
ipsl-cm4	1.70	0.31	0.18	0.22	0.60
cnrm-cm3	1.45	0.52	0.25	0.23	0.61
gfdl-cm2-1	2.28	0.33	0.19	0.17	0.74

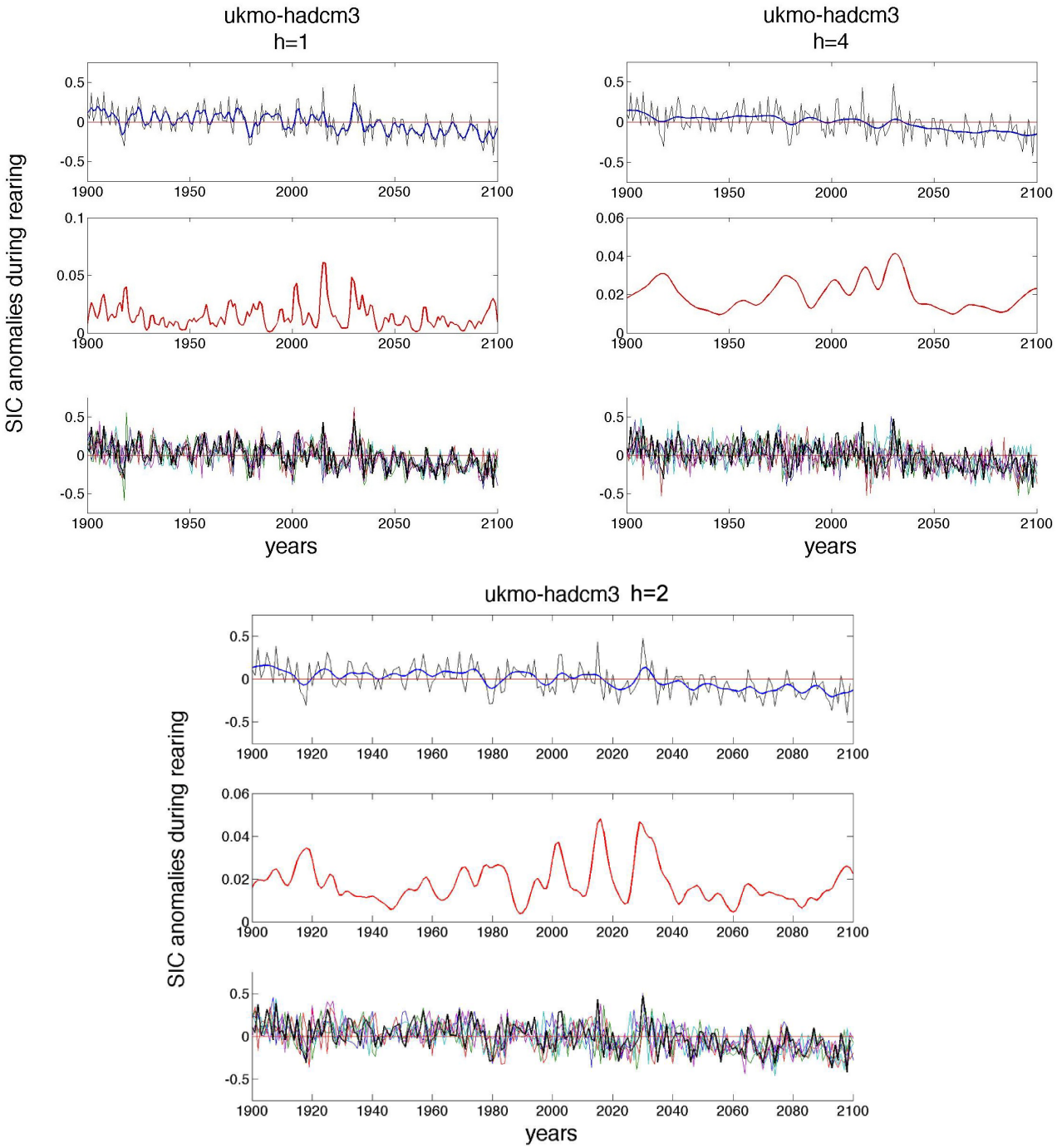

Figure 12: Smoothed mean (upper panel, blue line) of the SIC_a projected by the climate model ukmo-hadcm3 during the rearing season (black line) and smoothed variance (middle panel). The lower panel shows 5 stochastic forecasts (colored lines) obtained using different smoother parameters of the gaussian kernel filter, noted h. In our analysis we used $h = 2$.

6 Appendix 6: Vital rates projections

According to the GCMs, future SIC_a values will exceed the range observed during 1979-2007. We used the estimated functional relationships between SIC_a and the vital rates to project breeding success and adult survival in the future. During the last 6 decades, yearly breeding success ranged from 3% to 86% and annual adult survival from 60% to 98% (Barbraud and Weimerskirch 2001, Jenouvrier et al. 2005a). Figure 13 shows that the range of variation in the forecast vital rates from 2010 to 2100 is plausible.

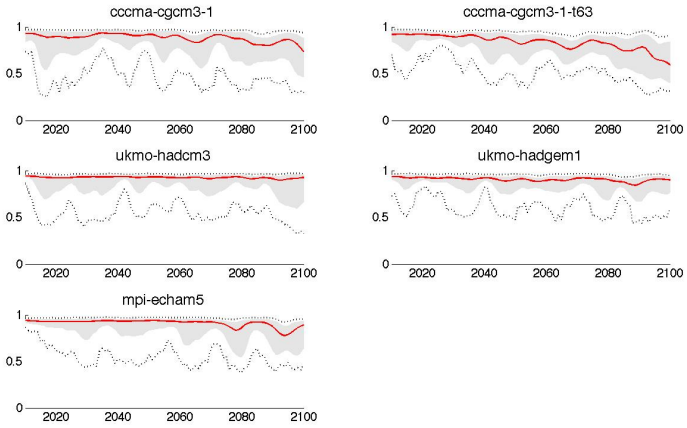

(a) Female survival

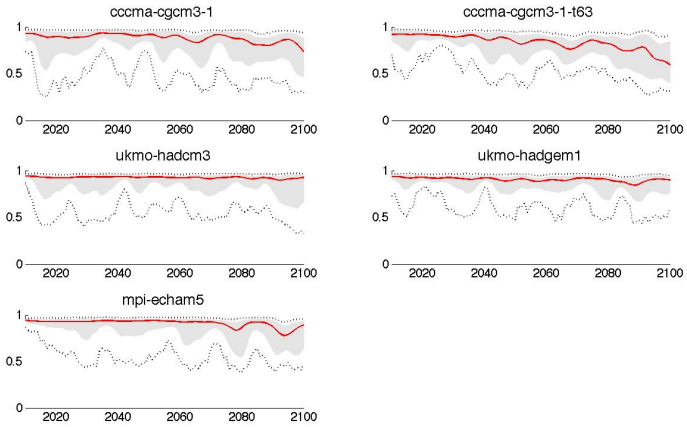

(b) Male survival

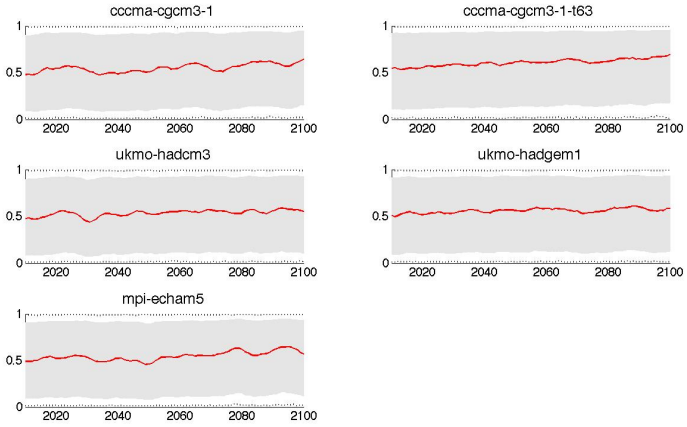

(c) Breeding success

Figure 13: Projection of vital rates of emperor penguins using SIC_a forecasts from five climate models from 2010 to 2100. The grey area shows the 95% envelope of 10000 simulations, the red line is the median, the dotted lines are the minimum and maximum simulated.

References

Ainley D, Russell J, Jenouvrier S, Woehler E, Lyver P, Fraser W, Kooyman G (2010) Antarctic penguin response to habitat change as earths troposphere reaches 2 degrees above preindustrial levels. *Ecological Monographs*, **80**, 49–66.

Barbraud C, Weimerskirch H (2001) Emperor penguins and climate change. *Nature*, **411**, 183–186.

Caswell H (2001) *Matrix population models*, vol. Second. Sinauer, Sunderland, Massachusetts.

Gimenez O, Barbraud C (2009) *Modeling Demographic Processes In Marked Populations Environmental and Ecological Statistics*, chap. The efficient semiparametric regression modeling of capture-recapture data: assessing the impact of climate on survival of two antarctic seabird species., pp. 43–58. Springer.

Jenouvrier S, Barbraud C, Weimerskirch H (2005a) Long-term contrasted responses to climate of two antarctic seabirds species. *Ecology*, **86**, 2889–2903.

Jenouvrier S, Weimerskirch H, Barbraud C, Park YH, Cazelles B (2005b) Evidence of a shift in cyclicity of antarctic seabirds dynamics link to climate. *Proceedings of the Royal Society of London.B.*, **272**, 887–895.